Flood Forecasting Experiment Based on EC and WRF in the Bailian River Basin

Zhiyuan YIN[1,2], Fang YANG[3*], Xiaohua LI[2]

1. China Meteorological Administration Basin Heavy Rainfall Key Laboratory/Hubei Key Laboratory for Heavy Rain Monitoring and Warning Research, Institute of Heavy Rain, China Meteorological Administration, Wuhan 430205, China; 2. Huanggang Meteorological Bureau of Hubei Province, Huanggang 438020, China; 3. Hubei Province Meteorological Information and Support Centre, Wuhan 430074, China

Abstract In order to extend the forecasting period of flood and improve the accuracy of flood forecasting, this paper took Bailian River Reservoir which located in Huanggang City of Hubei Province as an example and carried out basin flood simulation and forecasting by coupling the quantitative precipitation forecasting products of numerical forecast operation model of Institute of Heavy Rain in Wuhan (WRF) and the European Center for Medium-range Weather Forecasts (ECMWF) with the three water sources Xin'an River model. The experimental results showed that the spatiotemporal distribution of rainfall predicted by EC is closer to the actual situation compared to WRF; the efficiency coefficient and peak time difference of EC used for flood forecasting are comparable to WRF, but the average relative error of flood peaks is about 14% smaller than WRF. Overall, the precipitation forecasting products of the two numerical models can be used for flood forecasting in the Bailian River basin. Some forecasting indicators have certain reference value, and there is still significant room for improvement in the forecasting effects of the two models.

Key words Hydrometeor; EC; WRF; Xin'an River model; Bailian River

DOI 10.19547/j.issn2152 - 3940.2024.03.011

Flood disaster has always been one of the most serious natural disasters threatening human survival and development. The direct economic losses caused by floods in China reach tens of billions of yuan every year[1-2]. According to incomplete statistics, there are about 98 000 reservoirs in China, of which a considerable number of small- and medium-sized reservoirs have insufficient or even blank hydrometric stations. Such reservoirs often have large hidden dangers when facing local rainstorm and flood. Huanggang City is located in the eastern part of Hubei Province, with an overall terrain that gradually slopes from north to south. The northeastern border with Henan and Anhui is the Dabie Mountains, which originated from six major water systems including the Daoshui River, the Jushui River, the Bashui River, the Xishui River, the Qishui River, and the Huayang River, all of which flow through Huanggang City from north to south and join the Yangtze River. In June and July 2016, Huanggang City suffered severe floods with an average rainfall of nearly 700 mm. The affected population was 4.426 million, resulting in 19 deaths and 5 missing persons. The direct economic loss was 8.545 billion yuan. In the super Meiyu season of 2020, the total rainfall in Huanggang City exceeded that of 1998, ranking first in history and more than 60% higher than the average rainfall in Hubei Province. Floods and waterlogging disasters affected more than 1.35 million people in Huanggang City, with 81 000 hm^2 of crops affected and direct economic losses of nearly 750 million yuan[3].

With the continuous development of modern meteorological numerical forecasting models (hereinafter referred to as numerical models), the accuracy and frequency of rainfall forecasting are also increasing. It can effectively improve the accuracy of flood forecasting, strengthen the scientificity and predictability of reservoir flood control and scheduling, and ensure the reservoirs safety during flood season by using high-precision rainfall forecasting for watershed flood forecasting[4]. At present, many experts and scholars at home and abroad are coupling various numerical model forecasting products with different hydrological models to conduct experimental research on runoff simulation and flood forecasting[5-9]. Based on WRF and grid Xin'an River model, Gong Junchao *et al.*[10] carried out flood forecasting simulation for the Tunxi River basin, achieving high simulation accuracy. Huang Zequn *et al.*[11] combined the DRIVE-Urban model with rainfall data from automatic weather station to finely simulate two typical waterlogging events in the Changsha area, and hit rate of a waterlogging point was over 60%. Goodarzi *et al.*[12] coupled WRF with HEC-HMS model, and carried out flood forecasting experiment in the Talesh watershed of Iran, and the results showed that the coupling of meteorological and hydrological models can be used for flood forecasting in the region. Most of the existing research is conducted by coupling a numerical model with a hydrological model, and there is relatively little research on the comparative analysis of different numerical model forecast products in flood forecasting.

Received: May 4, 2024 Accepted: June 25, 2024

Supported by Open Project Fund of China Meteorological Administration Basin Heavy Rainfall Key Laboratory (2023BHR-Y26); Innovation Project Fund of Wuhan Metropolitan Area Meteorological Joint Science and Technology (WHCSQY202305); Innovation and Development Special Project of China Meteorological Administration (CXFZ2022J019); Project of Huanggang Meteorological Bureau's Scientific Research (2022Y02).

* Corresponding author.

Therefore, this paper attempted to couple two commonly used numerical models in meteorological operations with hydrological model, and selected the only large-scale reservoir in Huanggang City—Bailian River Reservoir as the research object to carry out basin flood forecasting experiment, providing scientific reference and technical support for flood control decision-making in the basin.

1 Data and methods

1.1 Overview of the basin The Bailian River Reservoir is located in the middle reaches of the Xishui River in eastern Hubei Province. It is the first artificial reservoir in eastern Hubei and a key water conservancy project in the Xishui River basin. It has begun to be built in the autumn of 1958, and the main dam was used for flood control and water storage in October 1960. The controlled watershed area is 1 797 km^2, with a total storage capacity of 1.228 billion m^3, accounting for 82.6% of the total water storage in the watershed. There are 28 meteorological observation stations distributed in the watershed, which is a multifunctional reservoir mainly for irrigation and power generation, while also considering flood control, fish farming, shipping, and comprehensive utilization (Fig. 1). The shape of the reservoir basin is long from north to south and narrow from east to west, with an average width of 15.7 km, slightly resembling the shape of banana leaves. The terrain is high in the northeast and low in the southwest. The Xishui River basin belongs to the subtropical monsoon climate zone, with a mild climate and an average annual temperature of 16.7 ℃. It is cold in winter and hot in summer, with distinct four seasons. This basin belongs to the rainstorm area in eastern Hubei, with the average annual rainfall of 1 366 mm. The spatial and temporal distribution of rainfall is uneven, concentrated between June and August. Rainstorm is frequent and intense, with steep rise and fall of flood and short convergence time.

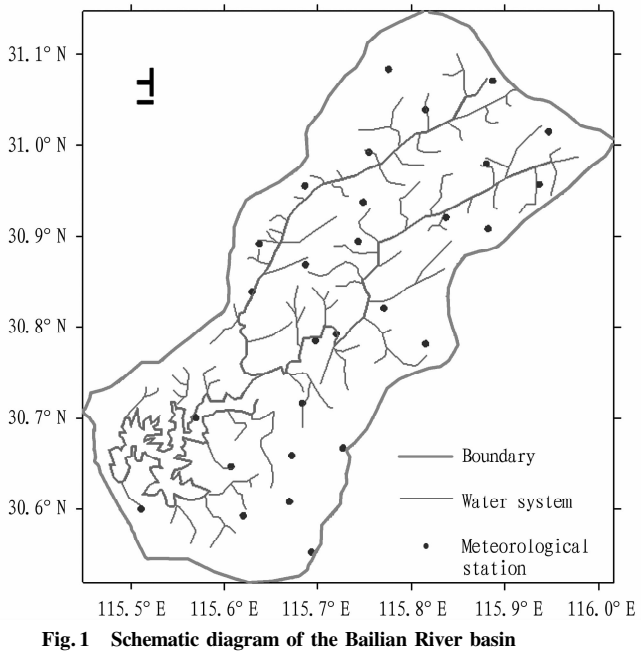

Fig. 1 Schematic diagram of the Bailian River basin

1.2 Research methods

1.2.1 Hydrological model. The Xin'an River model was proposed by Professor Zhao Renjun *et al.* from the former East China Institute of Water Resources[13], and was improved on the basis of modern slope hydrology to become the current three water sources Xin'an River model. The Xin'an River model is a decentralized structure that divides the watershed into many unit watersheds. For each unit watershed, the rainfall-runoff calculation is performed to obtain the outlet flow process of the unit watershed. Then, the river flood calculation below the outlet is carried out to obtain the flow process of the watershed outlet. The total outflow process of the watershed outlet is obtained by adding the outflow processes of each unit watershed. In recent decades, the Xin'an River model has been continuously improved and widely applied in humid and semi humid areas both domestically and internationally[14].

1.2.2 WRF model. Mesoscale numerical model WRF (Weather Research and Forecasting Model) was jointly developed by NCAR, NOAA, and multiple research institutions in the United States. This model integrates numerical weather forecasting, atmospheric simulation, and data assimilation, which can better improve the simulation and forecasting of mesoscale weather. Since the first version was launched in 2000, it has been applied and tested in multiple countries around the world, and has shown good forecasting ability for the intensity and falling zone of precipitation processes in multiple regions of China[15-18]. At present, the WRF model has been used as the operational forecasting model of the Central China Regional Numerical Forecasting Center, providing three layers of nested forecast products with two time intervals per day (00:00, 12:00 UTC), with a forecast time of 84 h. Among them, the first layer has a resolution of 27 km × 27 km, covering the whole country. The second layer has a resolution of 9 km × 9 km, covering the Central China region (Henan, Hubei, Hunan). The third layer has a resolution of 3 km × 3 km, covering Hubei Province and the Three Gorges Reservoir area. Based on previous research[19], the overall forecasting performance of the 9 km product is better than that of the 3 and 27 km products. Therefore, this study selected a rainfall forecasting product with a resolution of 9 km × 9 km to conduct forecasting experiments.

1.2.3 ECMWF model. The European Centre for Medium-range Weather Forecasts (ECMWF) is an international organization supported by 34 countries. It was officially established in 1975, and is headquartered in Bracknell, UK. EC mainly provides 10 d medium-term numerical forecast products, and also sends some useful medium-term numerical forecast products to all countries in the world through the global communication network maintained by the World Meteorological Organization (WMO). The model used fully utilizes four-dimensional assimilation data and can provide wind, temperature, and humidity forecasts for a total of 20, 911, and 680 points on a 40 km grid density with 60 layers at a height of 65 km worldwide. This project used EC forecast rainfall data with a spatial resolution of 0.125° × 0.125°, covering the range of 10° S – 60° N and 0° – 180° E, including analysis of various meteorological elements and forecast field data. The forecast time is up to 240 h (with a 3-hour interval within 72 hours and a 6-hour interval between 78 – 240 hours), and forecast products with two time in-

tervals are generated daily (00:00, 12:00 UTC). According to the actual test results in multiple regions of China, the rainfall forecast results of EC have all received high ratings[20-22].

1.3 Evaluation and inspection The evaluation of flood forecasting calculation results adopts three commonly used indicators in hydrological forecasting [*Hydrological Information Forecasting Specification* (GB/T 22482 - 2008)][23], namely the coefficient of certainty (DC), the relative error of flood peak (DQ), and the time difference of peak appearance (DT).

$$DC = 1 - \frac{\sum_{i=1}^{M}[y_c(i) - y_0(i)]^2}{\sum_{i=1}^{M}[y_c(i) - \bar{y}]^2} \quad (1)$$

$$DQ = \frac{|Q_{obv} - Q_{cal}|}{Q_{obv}} \times 100\% \quad (2)$$

$$DT = |TQ_{obv} - TQ_{cal}| \quad (3)$$

In the formulas (1) - (3), $y_c(i)$ is actual measured flood discharge value; $y_0(i)$ is the forecasted flood discharge value; $\bar{y}$ is mean of measured flood discharge sequence; Q_{obv} is measured flood peak discharge; Q_{cal} is simulated discharge; TQ_{cal} is peak occurrence time of forecasted flood peak discharge; TQ_{obv} is peak occurrence time of actual flood peak discharge. According to the *Hydrological Information Forecasting Specification* (GB/T 22482 - 2008), $DC > 0.5$, $|DQ| \leqslant 20\%$, $|DT| \leqslant 3$, the forecast result is qualified. Among them, $DC > 0.9$ is grade A forecast level; $0.9 \geqslant DC > 0.7$ is grade B forecast level; $0.7 \geqslant DC > 0.5$ is grade C forecast level.

2 Results and analysis

2.1 Historical case inversion By selecting 7 flood processes from 2013 to 2016, the model parameters were optimized and calibrated, and then 4 flood processes from 2020 to 2021 were used to test the model. According to Table 1, the average efficiency coefficient of the calibration period was 85.61%, the average relative error of the peak was 15.49%, and the average peak occurrence time difference was 1 h; the average efficiency coefficient during the verification period was 79.13%, the average relative error of the flood peak was 9.48%, and the average peak occurrence time difference was 1.4 h. Overall, the efficiency coefficient and relative error of the flood peak during the calibration period were higher than those during the verification period, and the time difference of peak occurrence was slightly lower than that during the verification period. The calculation accuracy of both has reached the level of Grade B forecasting. Fig. 2 was obtained by interpolation of 72 h cumulative rainfall of station in the validation period combined with the inverse distance square method. The 72 h cumulative average rainfall of the four processes was 49.3, 299.7, 76.7 and 60.0 mm, respectively. Among them, event 20200718 had the largest rainfall intensity, reaching the magnitude of extremely heavy rainstorm (24 h cumulative rainfall was more than 250 mm).

Table 1 Results of Xin'an River model during calibration and validation periods

Period	No.	Average cumulative rainfall//mm	Actual measured flood peak//m^3/s	Simulated flood peak//m^3/s	DC//%	DQ//%	DT//h
Calibration	20130606	102.4	733	711	89.72	2.92	3.0
	20130705	232.6	2 530	2 779	81.75	9.89	1.0
	20140704	90.1	852	1 083	78.41	27.10	1.0
	20150514	89.3	2 038	2 059	94.43	1.03	0
	20150616	137.7	3 319	2 942	83.25	11.35	1.0
	20150722	81.9	1 561	2 148	77.78	37.66	1.0
	20160618	108.6	2 823	2 301	93.91	18.47	0
	Absolute average	120.4	1 979	2 003	85.61	15.49	1.0
Validation	20200701	49.3	1 023	959	88.64	6.19	0
	20200704	299.7	4 698	5 240	78.89	11.54	2.0
	20200718	76.7	1 177	1 290	72.56	9.59	0
	20210703	60.0	920	878	69.94	4.62	4.0
	Absolute average	105.7	1 955	2 092	79.13	9.48	1.4

2.2 EC flood forecast test results Comparing Fig. 2 with Fig. 3, from the spatial distribution of rainfall, the distribution of heavy rainfall in the three processes of 20200701, 20200704, and 20210703 was basically consistent with the actual situation. However, the coverage area of heavy rainfall was smaller than the actual situation, resulting in a 6.90%, 14.11%, and 14.83% lower cumulative average rainfall forecast for the watershed. The spatial distribution of rainfall for the event 20200718 was significantly different from the actual situation. The heavy rainfall area was located at the southern end of the basin, completely opposite to the actual distribution. The maximum cumulative rainfall exceeded 250 mm, but the coverage area was smaller than the actual situation. The final average cumulative rainfall of the basin was close to the actual situation, with a relative error of 4.56%.

From the three forecast indicators in Table 2, the average efficiency coefficient was about 16% lower than the accuracy during the validation period. Among the four processes, the efficiency coefficients of three processes were above 60%, and the efficiency coefficient of one process was around 50%. The relative error of the flood peak was below 20%, and the average error did not ex-

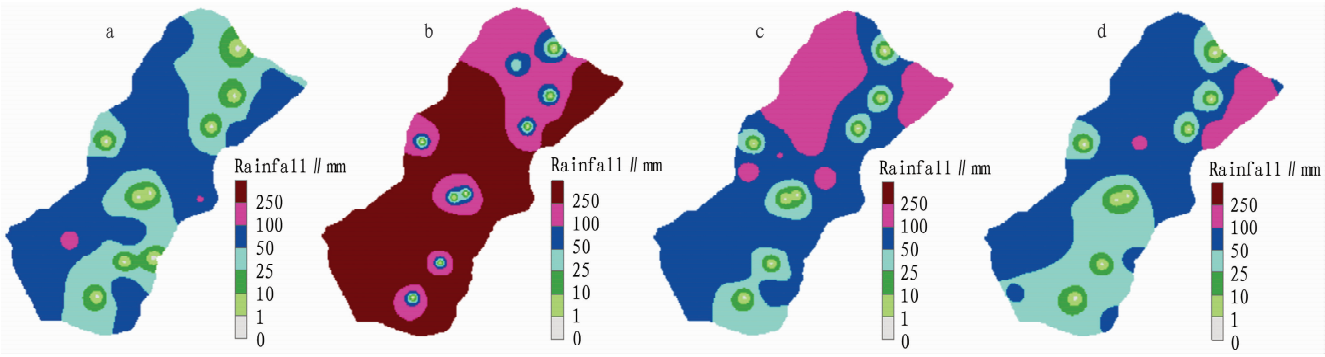

Note: a. 2020070109; b. 2020070421; c. 2020071821; d. 2021070321.

Fig. 2 72 h accumulated actual rainfall during the verification period

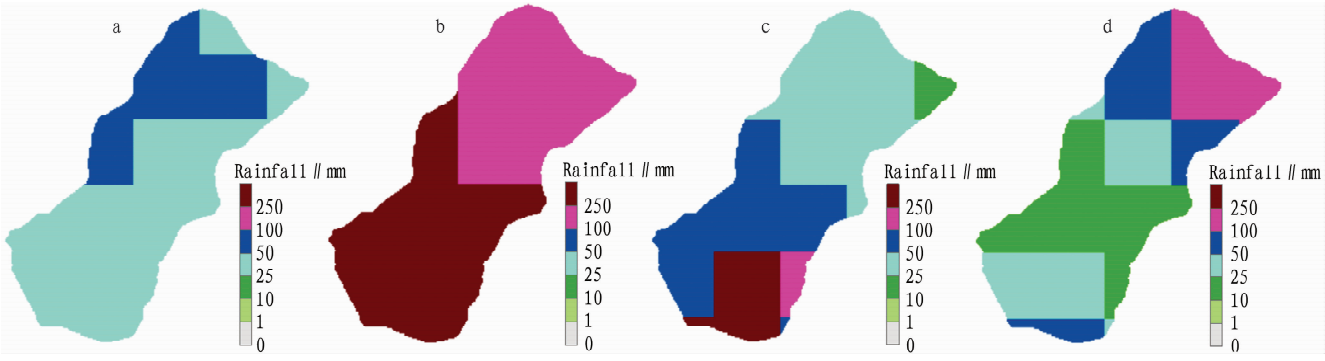

Note: a. 20200701; b. 20200704; c. 20200718; d. 20210703.

Fig. 3 72 h cumulative rainfall of EC forecast during verification period

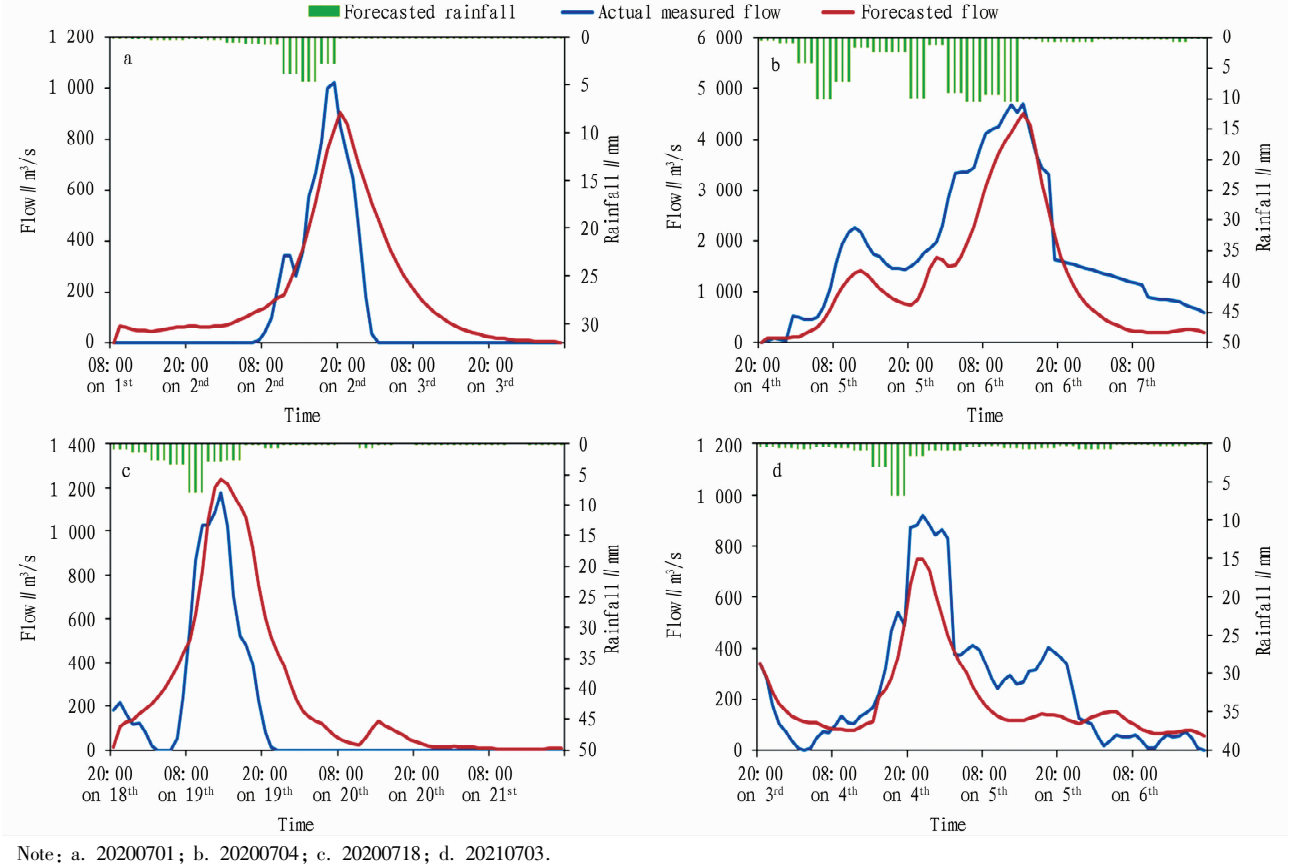

Note: a. 20200701; b. 20200704; c. 20200718; d. 20210703.

Fig. 4 Flood process predicted by EC

ceed 10%. The forecast accuracy of the peak arrival time difference was less than 1 h, which was consistent with the verification period. The overall forecast level was Class C, and the forecast results of the relative error of the flood peak and the time difference of peak occurrence were relatively close to the verification period. The low cumulative rainfall forecast of EC was the main reason for the low efficiency coefficient. In addition, it can be seen from Fig. 4 that the water rising stages of the four processes were in good agreement with the actual situation, but the water retention curve had a larger error compared to the actual situation, which may be related to the decrease in rainfall accuracy predicted by the numerical model with the extension of the forecast period.

Table 2 Various indicators of flood process predicted by EC

No.	Average cumulative rainfall // mm	Actual measured flood peak // m^3/s	Forecasted flood peak // m^3/s	DC // %	DQ // %	DT // h
20200701	45.9	1 023	905	63.54	11.520	1.0
20200704	257.4	4 698	4 507	69.19	4.062	0
20200718	73.2	1 177	1 240	50.63	5.310	0
20210703	51.1	920	748	72.05	18.740	1.0
Absolute average	106.9	1 955	1 850	63.85	9.910	0.5

2.3 Flood forecasting test results by WRF Comparing Fig. 2 with Fig. 5, from the spatial distribution of rainfall, it can be seen that the forecast results of the four processes were significantly different from the actual situation. The event 20200701 had a certain reflection of the rain falling area, and the distribution of heavy rainfall in the event 20200704 was partially similar to the actual situation, but the coverage area was significantly smaller. The heavy rain falling area in the event 20200718 was offset from the actual situation, and there was also a problem of smaller range. The heavy rain falling area in the event 20210703 was consistent with the actual situation, but the overall rainfall intensity in other parts of the basin was weaker. From the perspective of cumulative average rainfall in the basin, the relative errors of the three processes of 20200701, 20200718, and 20210703 were significantly smaller, with 22.11%, 42.63%, and 22.50% respectively. Only the relative error of 20200704 was 5.31%, which was relatively small. Seen from Fig. 6, for the rainfall process below 100 mm, the error of peak occurrence time was small, the predicted flood peak discharge was low, and the efficiency coefficient was not high. But for the rainfall process of extremely heavy rainstorm magnitude, the predicted flood peak discharge was relatively close to the actual situation, and the efficiency coefficient was also improved.

From the three forecast indicators in Table 3, the average efficiency coefficient was about 15% lower than the accuracy during the validation period. Among the four processes, the efficiency coefficients of two processes were above 70%, and the efficiency coefficient of one process was below 50%. The relative error of the average flood peak was 23.72% larger than that of the verification period. Only the flood peak forecast error of the event 20200704 process was relatively small, while the flood peak forecast errors of the other three processes were all above 20%. The average peak occurrence time difference was 0.75 h, which was consistent with the validation period. The overall forecast level was Class C, with the forecast results of peak arrival time difference being close to the validation period, and the efficiency coefficient being basically the same as EC. The forecast accuracy of flood peak was poor.

Table 3 Various indicators of flood process predicted by WRF

No.	Average cumulative rainfall // mm	Actual measured flood peak // m^3/s	Forecasted flood peak // m^3/s	DC // %	DQ // %	DT // h
20200701	38.4	1 023	744.0	84.59	27.25	1.00
20200704	283.8	4 698	4 959.0	58.14	5.56	0
20200718	44.0	1 177	759.0	73.41	35.55	1.00
20210703	46.5	920	676.0	41.85	26.51	1.00
Absolute average	103.2	1 955	1 784.5	64.49	23.72	0.75

2.4 Comparison of experimental results Whether in terms of spatial distribution of rainfall or cumulative values, the forecast results of EC were closer to reality compared to WRF. Moreover, the smaller the cumulative rainfall, the more obvious this difference becomes. Due to the differences in the spatiotemporal distribution of rainfall forecasts between EC and WRF, the average relative error of flood peaks in EC forecasts was about 14% lower than that in WRF forecasts. However, there was no significant difference between the two in terms of flood forecasting efficiency coefficient and peak occurrence time difference. Overall, the flood forecasting accuracy of EC was higher than that of WRF. Although the efficiency coefficients forecasted by the two numerical models were lower than 70%, they were within the allowable range of error in predicting the relative error of flood peaks and the peak occurrence time difference.

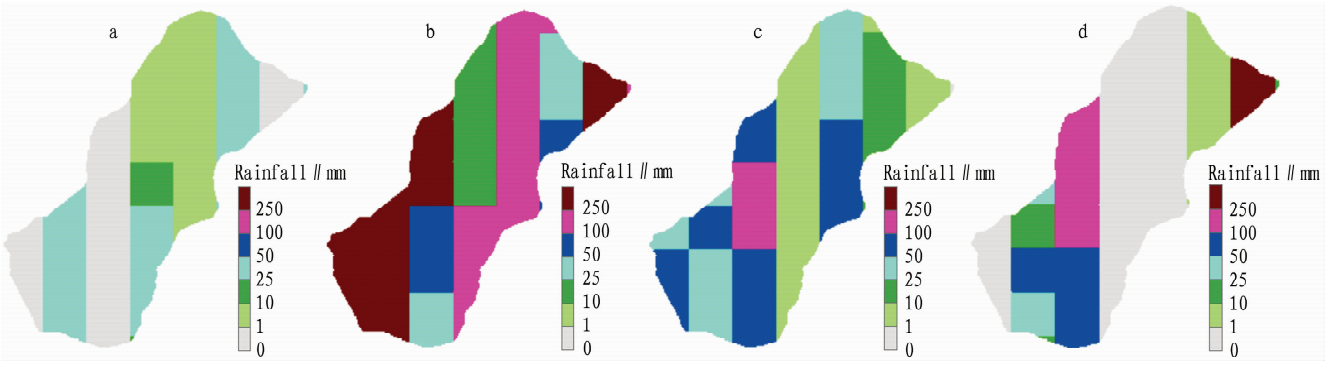

Note: a. 20200701; b. 20200704; c. 20200718; d. 20210703.

Fig. 5 72 h cumulative rainfall during verification period forecasted by WRF

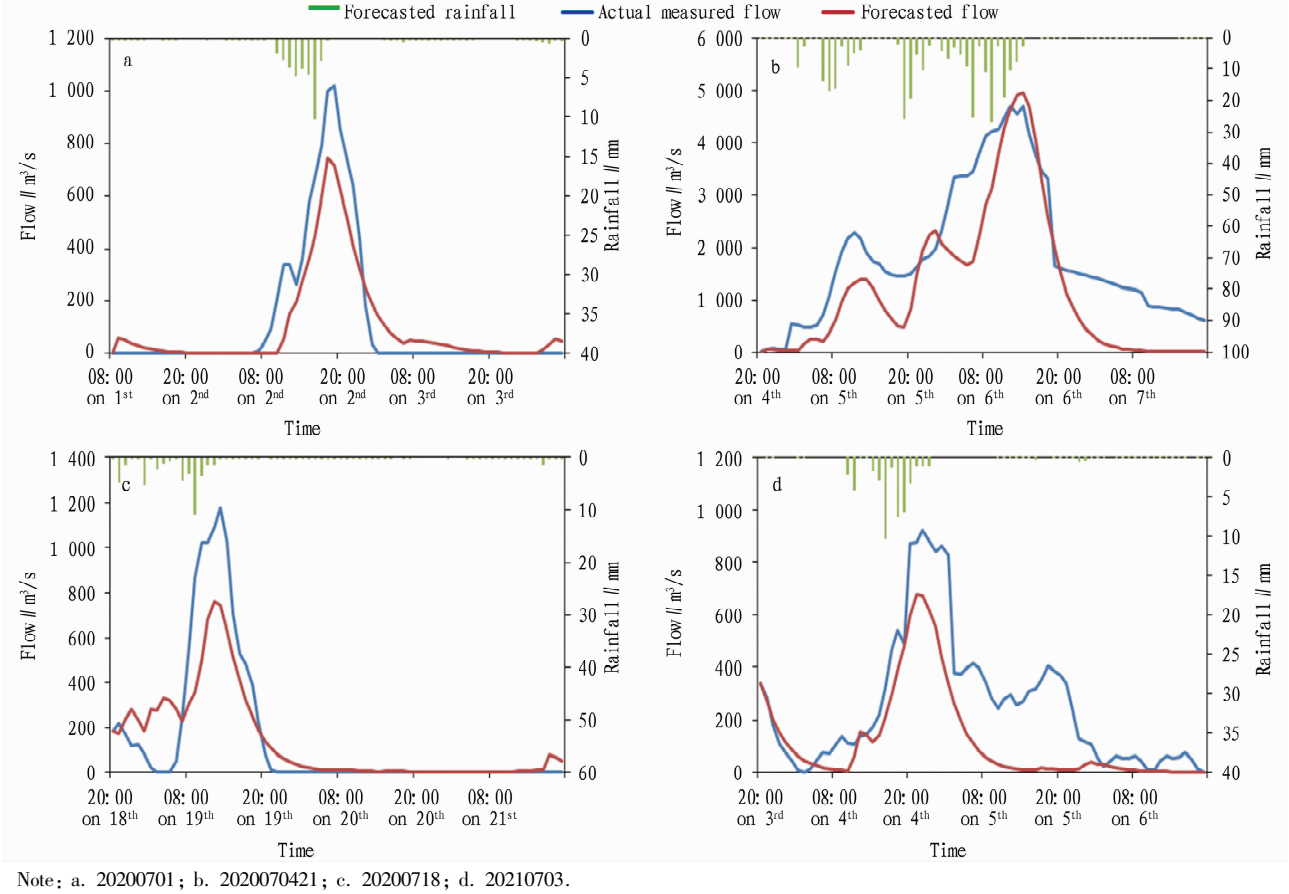

Note: a. 20200701; b. 2020070421; c. 20200718; d. 20210703.

Fig. 6 Flood process forecasted by WRF

3 Conclusions

(1) 11 flood processes in the Bailian River basin in the past 10 years were selected. Combining the Xin'an River model, flood forecasting experiments were conducted. Seen from simulation effects of historical cases, the average efficiency coefficient was about 80%, the average relative error of the flood peak was about 10%, and the peak occurrence time difference was 1 h, reaching the level of Class B forecasting. It can be used for flood forecasting in the Bailian River Reservoir during the flood season and provide reference for flood control decision-making.

(2) The rainfall forecasting products of EC and WRF numerical models were used in flood forecasting experiments. Through comparative analysis, it was found that EC's prediction of efficiency coefficient and peak occurrence time difference was basically the same as WRF, but the accuracy of flood peak prediction was about 14% higher than WRF. Overall, the forecasting experimental effect of EC on flood was better than WRF.

(3) On the one hand, although the overall effectiveness of rainfall forecasting products for flood forecasting in this study did not reach Class B or above, some indicators such as relative error of flood peak and peak occurrence time difference still had certain reference value for forecasting accuracy. With the continuous de-

velopment of numerical models, the accuracy of rainfall forecasting will also increase, and its application to flood forecasting will become better and better. This is also a trend of coupling hydrology and meteorology. On the other hand, due to the limited number of collected flood cases, there is still room for improvement in the effectiveness of model forecasting. In the later stage, with the collection and use of more flood data for process inversion, it will help improve the model parameter structure and further enhance the forecasting accuracy.

References

[1] National Major Natural Disasters Comprehensive Research Group of the National Science and Technology Commission. China major natural disasters and disaster reduction strategies (general)[M]. Beijing: Science Press, 1994.

[2] XIA J, WANG HY, GAN YY, *et al.* Research progress in forecasting methods of rainstorm and flood disaster in China[J]. Torrential Rain and Disasters, 2019, 38(5): 416 – 421.

[3] WANG FX, XU L, PENG DX. On the flood forecasting and dispatching of Bailianhe Reservoir[J]. Hydropower and New Energy, 2019, 33(5): 13 – 15.

[4] QU LY. Applicability of high-resolution numerical rainfall forecasts in flood forecasting over small and medium sized river basin[J]. China Flood & Drought Management, 2023, 33(6): 55 – 61, 87.

[5] JIN Q, WANG JZ, GAO Q, *et al.* Flood prediction system of Three Gorges Reservoir based on heavy rains forecast and its evaluation[J]. Journal of Catastrophology, 2012, 27(3): 54 – 58.

[6] CONG LY, GAO YF, PENG T, *et al.* Error propagation characteristics of WRF/WRF – hydrometeorological – hydrological coupling model: Taking the runoff forecasting in Zhanghe River basin as an example[J]. Journal of Tropical Meteorology, 2023, 39(6): 955 – 964.

[7] SONG SK, WANG HL, LANG ZL, *et al.* Mountain flood simulation of small basin in Taihang Mountains using HEC-HMS model: A case study of Luluochuan River basin[J]. Journal of Catastrophology, 2023, 38(1): 117 – 124.

[8] JIA YF, WU ZY, LI Y, *et al.* Research on forecast of flood rainstorm at kilometer scale in Haoxi Basin based on WRF model[J]. Water Resources and Power, 2024, 42(4): 6 – 9, 14.

[9] LIU YX, YUAN X, JIAO Y, *et al.* Ensemble forecasts of extreme flood events with weather forecasts, land surface modeling and deep learning[J]. Water, 2024, 16(7): 990.

[10] GONG JC, YAO C, SUN MK. The Grid-XAJ model driven by WRF model and its application[J]. China Rural Water and Hydropower, 2024(4): 24 – 33.

[11] HUANG ZQ, CHEN WT, LI YY, *et al.* Research of urban waterlogging in Changsha City based on DRIVE-urban model[J]. Journal of Catastrophology, 2024, 39(1): 104 – 108, 134.

[12] GOODARZI MR, POORATTAR MJ, VAZIRIAN M, *et al.* Evaluation of a weather forecasting model and HEC-HMS for flood forecasting: Case study of Talesh catchment[J]. Applied Water Science, 2024(14): 34.

[13] ZHAO RJ. Watershed hydrological model: The Xin'an River model and the northern Shaanxi model[M]. Beijing: Water Conservancy and Electric Power Press, 1984.

[14] SONG ZY. Xin'an River model application research in the absence data of Lengshui River basin[J]. Environmental Science & Technology, 2016, 39(S2): 488 – 492.

[15] GAO YF, WU YZ, WU YQ, *et al.* Rainfall-runoff simulation of Qingjiang River basin based on WRF model[J]. Journal of Tropical Meteorology, 2022, 38(5): 621 – 630.

[16] LIN SN, ZHANG YC, SUN S, *et al.* Sensitivity study of WRF parameterization schemes and initial fields on rainstorm simulation in Minjiang River basin[J]. Pearl River, 2023, 44(10): 35 – 46, 61.

[17] ZHOU ZM, WANG B, GUO YL, *et al.* Numerical simulation and analysis on cloud microphysical characteristics during a Meiyu heavy rainfall event in Hubei Province[J]. Torrential Rain and Disasters, 2023, 42(4): 372 – 383.

[18] ZHAO YT, XUE M, JIANG J, *et al.* Assessment of wet season precipitation in the central United States by the regional climate simulation of the WRFG member in NARCCAP and its relationship with large-scale circulation biases[J]. Advances in Atmospheric Sciences, 2024(41): 619 – 638.

[19] YIN ZY, WANG ZB, LI J, *et al.* An experimental study on the prediction of flood using coupled WRF-Topmodel model[J]. Acta Meteorologica Sinica, 2017, 75(4): 672 – 684.

[20] KONG XB, XIA XL, CU YK, *et al.* Verification of EC model's effect to forecast precipitation in Beipan River basin[J]. Pearl River, 2021, 42(5): 9 – 19.

[21] LONG KJ, KANG L, XIAO DX, *et al.* Correction method of heavy rainfall in the Sichuan Basin based on multi-model forecasting[J]. Torrential Rain and Disasters, 2024, 43(1): 54 – 62.

[22] ZHOU SN, WANG DY, FENG Y, *et al.* Verification and analysis of precipitation forecast during the Meiyu period of 2021 in Anhui Province[J]. Desert and Oasis Meteorology, 2024, 18(1): 165 – 173.

[23] Hydrological information forecasting specification (GB/T 22482 – 2008)[S].

(From page 52)

[7] LI C, WANG Y. The analysis and value of the community in industrial area in the early founding of P. R. China: Taking community in industrial area in Wuhan Honggangcheng as an example[J]. Chinese & Overseas Architecture, 2012(11): 70 – 72.

[8] GRAHAM B, ASHWORTH GJ, TUNBRIDGE JE. A geography of heritage: Power, culture and economy[M]. London: Arnold, 2000.

[9] HONG Y. A study on the value evaluation of workers' new villages as a heritage model of the 20th century: A case study of Shanghai City[D]. Shanghai: Tongji University, 2018.

[10] ZHAO HY. Self-organized renew phenomenon in hybrid historic neighborhoods update and its implications: Tanhualin Neighborhoods in Wuchang old city for example[J]. Decoration, 2015(7): 104 – 107.

[11] LIU DY. Naming heritage building thereafter[J]. Time + Architecture, 2001(4): 22 – 23.